Pharm Res (2012) 29:2456–2467
DOI 10.1007/s11095-012-0774-9

RESEARCH PAPER

Magnetised Thermo Responsive Lipid Vehicles for Targeted and Controlled Lung Drug Delivery

Dhrumil Upadhyay • Santo Scalia • Robert Vogel • Nial Wheate • Rania O. Salama • Paul M. Young • Daniela Traini • Wojciech Chrzanowski

Received: 16 December 2011 / Accepted: 1 May 2012 / Published online: 15 May 2012

ABSTRACT

Purpose Conditions such as lung cancer currently lack non-invasively targetable and controlled release topical inhalational therapies. Superparamagnetic iron-oxide nanoparticles (SPIONs) have shown promising results as a targetable therapy. We aimed to fabricate and test the *in-vitro* performance of particles with SPION and drug within a lipid matrix as a potentially targetable and thermo-sensitive inhalable drug-delivery system.

Methods Budesonide and SPIONs were incorporated into lipid particles using oil-in-water emulsification. Particles size, chemical composition, responsiveness to magnetic field, thermosensitiveness and inhalation performance *in-vitro* were investigated.

Results Particles of average diameter 2–4 μm with budesonide and SPIONs inside the lipid matrix responded to a magnetic field with 100% extraction at a distance of 5 mm. Formulations were shown to have accelerated rate of drug release at hyperthermic temperatures (45°C)—controlled release. The produced inhalation dry powder presented promising inhalation performance, with an inhalable fine particle fraction of 30%.

Conclusions The lipid system presented thermo-sensitive characteristics, suitable for controlled delivery, the model drug and SPION loaded lipid system was magnetically active and movable using simple permanent magnets, and the system demonstrates promise as an effective drug vehicle in targeted and controlled inhalation therapy.

KEY WORDS controlled drug delivery · inhalation · iron oxide · lipid · magneto-responsive · thermo-responsive · triggered drug release

ABBREVIATIONS

ABST	acrylonitrile butadiene styrene thermoplastic
AFM	atomic forced microscopy
DPI	dry powder for inhalation
DSC	differential scanning calorimetry
EDX	energy-dispersing X-ray analysis
HPMC	hydroxypropyl methylcellulose
Lip-Bud	budesonide containing lipid microcapsules
Lip-Bud-SPION	budesonide and SPION containing lipid microcapsules
Lipid	glyceryl behenate (Compritol 888)
logP	partition coefficient
SEM	scanning electron microscopy
SIOS	scanning ion occlusion sensing
SPION	superparamagnetic iron-oxide nanoparticles
XRD	X-ray diffraction

Electronic supplementary material The online version of this article (doi:10.1007/s11095-012-0774-9) contains supplementary material, which is available to authorized users.

D. Upadhyay · R. O. Salama · P. M. Young · D. Traini · W. Chrzanowski (✉)
The University of Sydney, The Faculty of Pharmacy
Pharmacy Building A15
Sydney, NSW 2006, Australia
e-mail: wchrzanowski@sydney.edu.au

S. Scalia
Department of Pharmaceutical Sciences, Ferrara University
44121 Ferrara, Italy

N. Wheate
Strathclyde Institute of Pharmacy and Biomedical Sciences
University of Strathclyde, 161 Cathedral Street
G4 0RE Glasgow, United Kingdom

R. Vogel
School of Mathematics and Physics, The University of Queensland
St Lucia, Qld 4072, Australia

R. O. Salama
Faculty of Pharmacy, University of Alexandria, Alexandria, Egypt

INTRODUCTION

Lung cancer is a highly prevalent disease associated with the uncontrolled growth of malignant cells (1). It is a leading cause of death worldwide (2) and affects humans of all race and gender. Lung cancer is associated with the highest mortality rate and is the 10th leading cause of deaths worldwide. It is expected to rank 5th within a few years due to its increasing prevalence in western countries (3).

Current chemotherapy treatments are neither specific, nor selective, for lung cancer (1,4). Inhalation is the most widely used route of administration of drugs for the majority of respiratory conditions, including asthma and chronic obstructive pulmonary disease (4,5). This route of administration may thus considered to be the most appropriate for delivery of anticancer agents.

Recent trials have shown increased drug concentration in cancerous cells and decreased systemic side effects after delivery of an inhaled anticancer agent (6). As lung cancer is often only associated with one side or one lobe of the lung, there is a concern that treatment may damage healthy parts of the lungs via even distribution of the inhaled chemotherapeutic (5).

Consequently, an enhanced method of targeted drug delivery to the lung is needed if the side-effects of systemic delivery are to be minimised. In the last few decades, the concept of magnetisation has shown some promising results in guiding drugs during therapy (7). The concept of magnetisation involves incorporating magnetically active particles to a chemotherapeutic drug, such that the particles, as well as the attached drug, can be guided to a specific location in the body using a strong external magnet (8,9). A range of pure metals and alloys can be used for this purpose including iron oxide, cobalt, nickel, platinum and magnesium (10). Apart from the type of metal used, the particle size is also important (7). Larger sized (above 500 nm) magnetite particles display magnetic hysteresis, which means that they remain magnetised even after an applied magnetic field has been removed (8). This is undesirable for targeted drug delivery (8). The size of such super paramagnetic iron oxide nanoparticles (SPIONs <100 nm) is also important in determining their distribution and clearance (7).

Biocompatible SPIONs such as magnetite have been widely used for *in vivo* biomedical applications including magnetic resonance imaging (MRI) contrast enhancement (11,12), tissue specific release of therapeutic agents (13), hyperthermia, and magnetic field assisted radionuclide therapy(14). Their slower renal clearance and higher relaxation values compared to the gadolinium-based contrast agents make them more attractive for imaging purposes (15). Drug-loaded SPIONs can be guided to the desired target area using an external magnetic field while simultaneously tracking the biodistribution of the particles (13,16). There were no long term consequences of using SPIONs identified in the literature (17). They have been so used because of their chemical stability, lack of toxicity and biodegradability. Iron oxide NPs will generate Fe^{2+} upon degradation, which can be well tolerated by cells up to certain levels (18). Importantly, they also have been taken through regulatory approval and may be safely, and legally, used in humans. These data suggest that SPIONs are biocompatible and do not cause any seriously, long term toxicity in humans, when administered intravenously (17,19).

In vivo studies have been carried out to characterise the side effects of SPIONs. So far, the only observed side effects of SPIONs include reversible greyish discolouration, which resolves in 7–14 days; lethargy; some urine discolouration without any irritation; transient increase in iron and ferritin levels without any clinical symptoms; and, accumulation of SPIONs in the liver for the first two days after treatment (19). Thus, although further studies are required, the SPIONs appear to be biocompatible and relatively non-toxic (17,19).

Apart from carrying the chemotherapeutic drug to its target site under the influence of a magnetic field, SPIONs can themselves be used for the destruction of tumours. When SPIONs are exposed to an alternating magnetic field the oscillation of the magnetic moment within the particles, and loss of magnetic hysteresis, release energy as heat to the surrounding tissues thus contributing to tumour cell death through hyperthermia (19,20).

Anticancer drugs can be susceptible to rapid chemical degradation, especially if formulated in aqueous media (5,6,21). This issue can be resolved by formulating SPION particles as dry powders for inhalation (22). In dry powder particles containing drug loosely bound SPIONs, the drug can easily dissociate the nanoparticles during delivery. It is therefore necessary to encapsulate both the drug and SPIONS into a microparticle formulation. Such a microparticle would remain intact until it reaches its target site and is broken open mechanically via electro-magnetically induced SPIONs oscillation.

Recently, a few studies have demonstrated the effectiveness of solid lipid microparticles in producing slow release formulations, especially for hydrophobic drugs (23,24). Glyceryl Behenate (lipid) is a solid at room temperature, with melting point of ~70°C, and a transition temperature (T_g) of 49°C, which may be desirable for controlling the release of encapsulated drug using SPION induced hyperthermia. Although extensive studies on the toxicology of lipids are lacking, *in vivo* studies have shown no significant increase in inflammatory mediators in the lungs after lipid administration (25,26).

The primary aim of this study was therefore to develop a method for the formulation of lipid microparticles containing a model drug and SPION as a dry powder inhaler (DPI)

formulation. The physical and chemical characteristics of the micro-particles were examined, as well as their performance as an inhalable and targetable formulation with thermally controlled drug release.

MATERIALS AND METHODS

Magnetically targetable and inhalable formulations have to fulfil several requirements that relate to size, chemistry, dry powder performance and mobility of the particles under external signals. Therefore, to achieve this aim, the study was designed and conducted in five main steps: (1) formulation of the particles of inhalation size, (2) drug formulation and its release profile, (3) assessment of magnetic mobility of the particles as a function of distance from the magnet, (4) evaluation of the thermally controlled drug release and, (5) aerosol performance of the dry powder formulation.

Materials

Micronised budesonide was supplied by Yicheng Chemical Corp (Jiangsu, China). Glycerol Behenate (Compritol 888) was obtained from Gattefossè SAS (Saint-Priest Cedex, France). Pluronic F-68 and phosphate buffered saline tablets were supplied by Sigma Aldrich (St. Louis, USA). Superparamagnetic Iron-Oxide Nanoparticles of average size 20–30 nm, were supplied by Nanostructured & Amorphous Materials, Inc (Houston, USA). Methanol (HPLC grade) was supplied by Lab-Scan Analytical Sciences (Bangkok, Thailand). Aqueous silicone coated release paper was purchased from Cotek Papers Ltd, UK. N38-grade, 30×10×6 mm neodymium magnets were purchased from the Aussie Magnet Company Pty Ltd (Australia).

Preparation of Drug-Loaded Lipid Microcapsules

Lipid microparticles containing budesonide (Lip-Bud) were produced using an oil-in-water (*o/w*) emulsification technique following the method described by Mezzena *et al.* (24). Budesonide was used as a model drug. It is commonly used as an inhaled medicine and is hydrophobic in nature. It has similar properties to chemotherapeutic drugs (e.g. Paclitaxel).

In brief, 0.16 mg budesonide was dissolved in 4 g of melted lipid at 90°C. This 4% *w/w* concentration of budesonide in lipid was chosen to deliver a therapeutic dose of 400 μg of budesonide for every 10 mg of the formulation inhaled, (equivalent to commercially available budesonide formulations). 50 mL of water containing 150 mg Pluronic F-68 (0.3% *w/v*) as surfactant, was also heated to 90°C and added to the lipid phase, causing a phase inversion to form the *o/w* emulsion. The mixture was then stirred at 10,000 rpm for 2 min at 90°C using a L4RT Silverstone Machine (Fast stirred sample) In order to see the effect of stirring speed on particle size, a second set of samples were prepared at a speed of only 5,000 rpm (slow stirred sample).

The fast and slow stirred microparticles were then rapidly cooled to room temperature using an ice bath, to solidify the lipid microcapsules. The mixtures were then frozen in liquid nitrogen and freeze-dried (20°C, 0.08 mbar pressure) for 48 h in Christ Alpha 1–4 freeze-dryer. The resultant dry powder was jet-milled to achieve a suitable particle size for inhalation delivery (<6 μm (27)). For method optimisation of both fast and slow stirred samples, and comparison purposes, one sample was not milled and one was only hand-milled (referred to as 'unmilled' and 'hand-milled' samples, respectively). All samples were then stored at 4°C and 10% relative humidity until required.

Budesonide and SPION containing lipid microparticles (Lip-Bud-SPION) were produced using the same methods as above, with 100 mg of SPIONs (5% *w/w*) suspended into the melted lipid in addition to budesonide. The Lip-Bud-SPION samples were stirred only at 10,000 rpm and were jet-milled following lyophilisation.

Detection of SPIONs in Microparticles by SEM and EDX

DPI samples were dispersed onto carbon sticky tabs and were gold coated to a thickness of approximately 20 nm. Scanning electron micoscropy (SEM) was performed at 2–5 keV using a Zeiss Ultra *plus* and Intellectual Quemscan Zeiss EVO 50. The presence of SPIONS iron nanoparticles within the Lip-Bud-SPION microparticles was also determined using elemental (Fe) maps by energy dispensing X-ray analysis (EDX). The experiments were conducted using a Zeiss Ultra *plus* system at 15 keV.

Determination of Microparticle Size

The size of the Lip-Bud and Lip-Bud-SPION microparticles was analysed as DPI samples using laser diffraction on a Malvern Mastersizer 2000. Samples were dispersed in a Scirocco dry dispersion unit and analysed in triplicate. Microparticle size was also analysed using Scanning ion occlusion sensing (SIOS) on a qNano machine. Samples were dispersed in phosphate buffer saline (PBS) and sonicated for 5 min to break down agglomerates. The instrument was calibrated using 6 μm polystyrene particles.

Determination of Microparticle Surface Characteristics

The topography of Lip-Bud and Lip-Bud-SPION microparticles were studied using non-contact mode atomic force microscopy (Park System XE-70). Samples were scanned with

silicon probe of conical shape; tip radius of curvature ~10 nm; tip length ~20 μm; force constant 45 (N/m); resonance frequency 335 kHz.

Chemical, Structural, and Thermal Analyses

Raman Spectroscopy

Raman spectroscopy was carried out on samples of lipid, budesonide, Lip-Bud and Lip-Bud-SPION using a inVia Renishaw Raman system at an operating wavelength of 488 nm. The spectra were acquired for 10 s from 99 to 3200 cm^{-1}.

X-Ray Diffraction (XRD)

X-ray diffraction patterns of lipid, budesonide, Lip-Bud and Lip-Bud-SPIONs were analysed using a Shimadzu S6000 XRD system. Samples were flattened on an aluminium specimen stage before measurements were taken using Cu Kα radiation at 30 mA and 40 kV and with an angular increment of 0.02°/s. Each analysis was measured in the range of 5–30 2θ.

Differential Scanning Calorimetry (DSC)

Thermal analysis was performed on lipid, Lip-Bud and Lip-Bud-SPION dry powders, using differential scanning calorimetry (Mettler-Toledo, Schwerzenbach, Switzerland). Approximately 5 mg of each powder was accurately weighed into a DSC pans and analysed from 0–300°C using a ramp rate of 10°C/min.

Magnetic Mobility Test

Mobility of Lip-Bud-SPION microparticles under an applied magnetic field was tested over a distance of 5–20 mm (Fig. 1). Approximately 10 mg of accurately weighed Lip-Bud-SPION was placed on a biocompatible aqueous silicone coated release paper, which has very low resistance and low reactivity with materials. The paper was then placed on a 5 cm high non-metallic, rubber platform. A rectangular acrylonitrile butadiene styrene thermoplastic sheet of 5 mm thickness was placed at minimum distance from the powder before three rare-earth magnets, each with surface magnetic force of 2194 gauss and pull strength of 4 kg, were then placed directly behind the thermoplastic sheet. The magnetic field was applied to the Lip-Bud-SPION microparticles for a period of 1 min during which time they were attracted to the thermoplastic sheet. The weight of powder remaining on the paper was then measured. The same process was carried out at distances of 10, 15 and 20 mm by stacking 2, 3 and 4 thermoplastic sheets of 5 mm each, respectively.

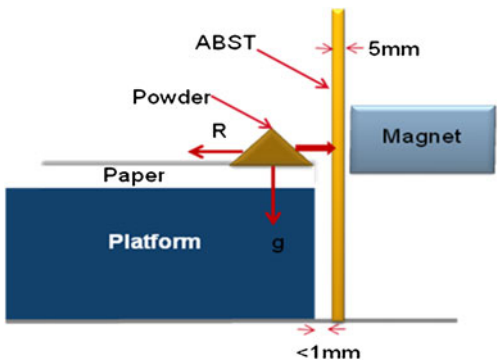

Fig. 1 Apparatus set up for magnetic mobility test over a distance of 5–20 mm.

In Vitro Diffusion/Dissolution

A modified British Pharmacopeia apparatus 4 (flow through cell) was used to assess budesonide release from microparticles containing only budesonide, Lip-Bud and Lip-Bud-SPION particles (24,28). Approximately 1 mg of budesonide microcapsules, 25 mg of Lip-Bud and Lip-Bud-SPION microparticles were accurately weighed and sandwiched between two 0.2 μm nylon membrane disc filters which had a diameter of 25 mm. The assembly was then secured in a filter adapter by plastic mesh screens. 50 mL of PBS was passed through the assembly at the rate of approximately 5 mL/min, in a closed loop system. Flow direction was maintained vertically to avoid dead volume. Aliquots of the PBS solutions (2 mL) were taken at various time points and replaced with 2 mL of fresh PBS each time. Phosphate buffer solution was used as the media instead of simulated lung fluid as it has already been shown by the authors that no statistical difference in budesonide release rate between these two media exists (29,30).

Budesonide drug concentration was determined by high pressure liquid chromatography (HPLC) on a Shimadzu HPLC system using a Waters Nova-pack® C18 column. with a detection wavelength of 240 nm, a flow rate of 1 mL/min, an injection volume of 100 μL, and a mobile phase of 60:40 methanol:water solution. A calibration graph between 1–100 μg/L was established using five points.

In Vitro Dry Powder Aerosol Performance

The aerosolisation efficacy of Lip-Bud-SPION microparticles was tested using the Marple-Miller cascade impactor (31). Size 3 hydroxypropyl methylcellulose (HPMC) capsules, each containing 11 mg of Lip-Bud-SPION microparticles were placed one at a time into the Aeroliser DPI device. The device was then activated, connected to a mouth-piece adaptor and tested

for 4 s at 60 L/min. The device, HPMC capsule, adaptor and filter were then washed with 15, 10, 5 and 5 mL of methanol, respectively, into separate volumetric flasks. Additional volumes of 5, 10, 10, 10, and 5 mL of methanol were then accurately placed into impactor stages 1, 2, 3, 4, and 5, respectively. The volumetric flasks and each stage were sonicated for 15 min to ensure destruction of the microcapules and dissolution of budesonide. An aliquot from each volumetric flask and stage collectors (1.5 mL) was centrifuged for 10 min for removal of solid lipid and silicone particles. The supernatant, containing dissolved budesonide, was then filtered through a 0.45 μm filter and analysed by HPLC for drug quantification (HPLC measurements as above). All analyses were performed in triplicate.

RESULTS AND DISCUSSION

In this work a novel inhalation delivery system, containing enhanced chemotherapy agents formulated around superparamagnetic iron nanoparticles encapsulated within lipid microcapsules, has been presented. Budesonide, an inhalable corticosteroid commonly used for asthma therapy, was used as a model drug because it has similar surface energy, logP and solubility to Paclitexel (Budesonide: logP=2.42, solubility $4.57e^{-02}$ g/l, Paclitaxe: logP=3.0, solubility $5.56e^{-03}$ g/l), even though is not a chemotherapeutic drug itself. The main reason for using budesonide instead of the actual chemotherapy agent its due to mainly to safety concerns following of exposure during the experiments, especially during jet milling and aerosol performance testing.

Microparticles containing budesonide (Lip-Bud) and microparticles containing both budesonide and SPIONS (Lip-Bud-SPION) were produced using an adaption of an oil-in-water method. The effect of emulsification condition i.e. stirring speed (high: 10000; low, 5000 rpm) and milling (hand-milled or jet milled) on the size, shape and structural integrity were examined.

Particle and Micoparticle Sizing

Budesonide

Samples of free budnesonide, empty lipid microcapsules, Lip-Bud and Lip-Bud-SPION were analysed using a number of different techniques to determined particle size and shape. The basic shape and size and particles morphology was examined using SEM. Budesonide particles appeared spherical with slightly rough surface and size of about 2 μm (Fig. 2). In contrast, SEM images of the unmilled sample (Lip-Bud) showed large string-like particle agglomerates with very few individual spherical particles – Fig. 2b. The high aspect ratio agglomerates had an average length of more than 20 μm. Hand-milled sample largely consisted of damaged lipid particles with very irregular and non-consistent shapes and particle sizes.

Slow stirred sample had spherical shape, smooth surface and average diameter of 10 μm, which was too large for inhalation therapy, thus only high speed stirring was used for all further formulation.

Lip-Bud formulation (produced using high speed stirring) also had relatively smooth surfaces and spherical shape, but the average diameter was 3–4 μm. A further drop in diameter to 2–3 μm was observed for Lip-Bud-SPION formulation, which also presented similar smooth morphology and spherical shape.

Both drug (Lip-Bud), and drug + iron nanoparticles (Lip-Bud-SPION) loaded lipid particles were successfully manufactured using emulsification technique. Conditions of the particles fabrication affected particles size distribution. The higher particle size of slow stirred sample compared to fast stirred Lip-Bud and Lip-Bud-SPION samples was expected as higher stirring speed increases the particle-particle and particle-wall collisions which results in higher droplet breakage and thus lower particle size after drying (32–34). These results also suggest that Jet-milling does not break the lipid particles formed during emulsification to cause decrease in original particle size; rather, it only de-agglomerates the particles, as otherwise, all particles would have the same size following jet-milling.

Microparticle Uniformity

The uniformity of the particle size distributions of both Lip-Bud and Lip-Bud-SPION were examined using laser diffraction and scanning ion occlusion sensing. Hand-milled sample of Lip-Bud and Lip-Bud-SPION had the widest size distribution with average diameter size of 7.3 μm (Fig. 3).

The slow stirred sample of Lip-Bud had a median diameter of 7.5 μm. Lip-Bud and Lip-Bud-SPION microparticles had median diameters of 3.2 μm and 2.9 μm, respectively, as well as a narrow range of size distributions of only 1.2 and 1.5 μm, respectively. These particle sizes were only slightly higher than that of micronised budesonide, which had an average particle diameter of 1.5 μm.

SIOS uses a tuneable elastomeric pore to detect the passage of nano- and micron- sized particles as a drop in ionic current across the pores (35–37). SIOS has recently been shown to be a fast and accurate method for single particle sizing (38). The mode and mean diameters were measured to be approximately 2.2 μm and 1.6 μm for Lib-Bud particles and 2.8 μm and 1.8 μm for Lip-Bud-SPION particles. It is of interest that the small peak at 6 μm in the particle distribution of Lip-Bud-SPION particles is due to a small residual trace of calibration particles.

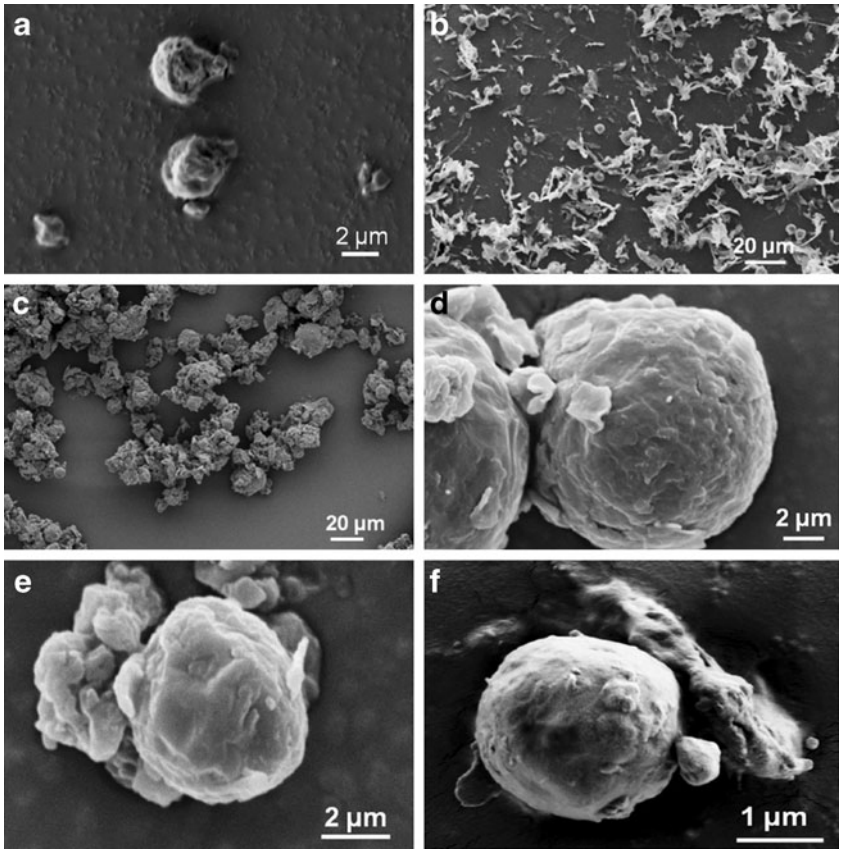

Fig. 2 Scanning electron microscope images of (**a**) budesonide, (**b**) unmilled sample of Lip-Bud, (**c**) Lip-Bud hand-milled sample, (**d**) Lip-Bud slow-stirred sample, (**e**) Lip-Bud and (**f**) Lip-Bud-SPION microparticles.

The results of particles sizing using different methods were inconsistent. Typically, sizes were smaller when measured using SIOS. These differences could be due to measurement errors (at least 10% for both methods) or particle aggregation. Laser diffraction peaks (for Lip-Bud and Lip-Bud-Spion) and SIOS distribution plots were similarly broad and particles of greater sizes were detected. These graphs indicated that samples could contain some aggregates, with some more aggregated than the other. Aggregation can be decreased in low concentration electrolytes as used in SIOS, hence smaller average particles size. In general, Lip-Bud-SPION particles had smaller average diameter than Lip-Bud particles when measured with laser diffraction, while the opposite was observed when sizes were measured using SIOS. It is likely that, due to the different methodologies used, intra-variations could affect results. Since the same particle preparation method was used, average diameter of both formulations was expected to be similar.

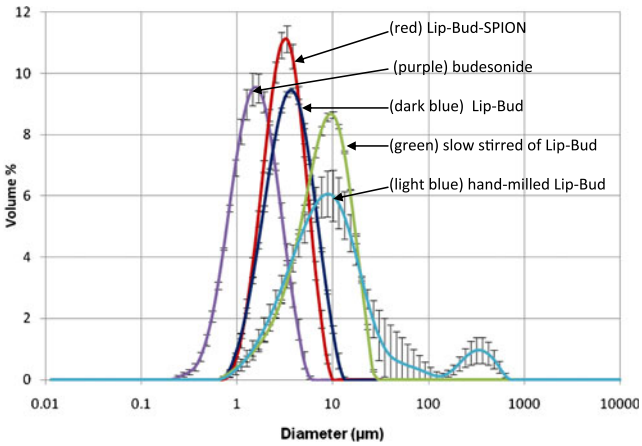

Fig. 3 Particle size distributions by laser diffraction (n=3) of (purple) budesonide only, (dark blue) Lip-Bud, (red) Lip-Bud-SPION, (green) slow stirred of Lip-Bud and (light blue) hand-milled Lip-Bud.

Some differences in sizes could be attributed to the change in mass of the particle, due to the incorporation of the SPIONS, which consequently could have an effect on the jet-milling process.

SEM data are not fully representative to analyze size distribution due to limited number of particles measured but they further confirmed sizes of the particles. It is important to notice that for inhalation purposes sizes below 5 µm are preferred and this size was achieved and confirmed with above techniques.

Atomic Force Microscopy (AFM)

Atomic force microscopy was used to examine the three-dimensional topography of the Lip-Bud and Lip-Bud-SPION microcapsules. The Lip-Bud particles were approximately 2 µm high and 2 µm wide, which suggest a regular spherical shape (Fig. 4). The topography reveals no large or sharp peaks,

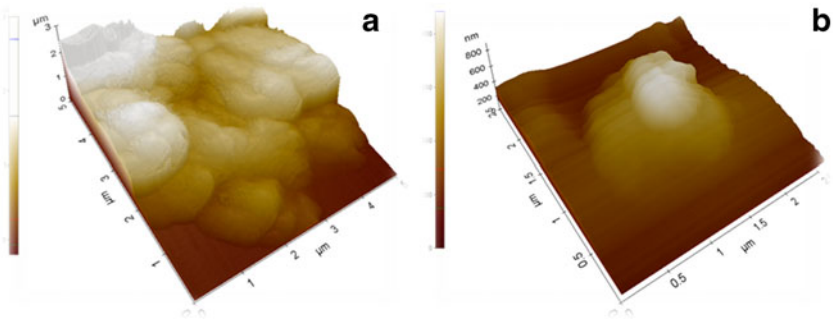

Fig. 4 3-Dimentional AFM topography images of (**a**) Lip-Bud and (**b**) Lip-Bud-SPION micro-particles showing smooth surfaces.

which suggests a primarily smooth morphology. Topography images of Lip-Bud-SPION, in Fig. 4b, shows similar results with a spherical particle of roughly 2 μm size, with smooth surface.

Chemical, Structural, and Thermal Analyses

The presence of budesonide in the microparticles was confirmed via variety of solid state techniques including Raman spectroscopy, X-ray powder diffraction, differential scanning calorimetry and energy-dispersing X-ray analysis. Raman spectrum of the free budesonide showed to have a strong peak at 1653 cm^{-1}, corresponding to the drug's quinonoid aromatic ring C=C bond vibration. Other small peaks at 1621, 1598 and 1448 cm^{-1} are attributed to aromatic C=O, C=C and aliphatic CH_3 or CH_2 vibrations respectively (Fig. 5), which are consistent with those reported for the drug (39). In particular following peaks were identified which corresponded to budesonide 3032 cm^{-1} aromatic CH stretching, 3007 cm^{-1} (C=CH) stretching, 2964 cm^{-1} CH_3, CH_2 stretching, 2929 cm^{-1} CH_2 stretching 2900 cm^{-1} CH_3 stretching, 1687 cm^{-1} (C=O), 1665 cm^{-1} (C=C), 1285 cm^{-1} (C–C), 1067 cm^{-1} and 1018 cm^{-1} C–OH stretching, 892 cm^{-1} OOC/CCH aromatic deformation. The Raman spectrum of empty lipid microparticles shows clear peaks at 869, 1060, 1129, 1294, 1417, 1437, 1443, 2694, 2844 and 2881 cm^{-1}. These peak positions and characteristics closely match that described for this lipid (40).

Finally, the Raman spectra of both Lip-Bud and Lip-Bud-SPION microparticles shows many clear peaks corresponding to lipid. A less sharp, but clear, peak was observed in both these samples at 1653 cm^{-1}, which confirms the presence of incorporated budesonide.

The results of X-ray diffraction confirmed the presence of budesonide inside the microparticles (Fig. 6). The two most intense and sharp peaks were seen at ~15 and 16 2θ and ~21 and 23 2θ, for budesonide and lipid respectively, with the number and position of the peaks consistent with literature values (24,41). Samples of Lip-Bud and Lip-Bud-SPION microparticles showed less sharp, but clear peaks corresponding to 15 and 16 2θ peaks of budesonide, and lipid peaks at 21 and 23 2θ were also observed with an additional small peak at 19 2θ.

Thermal analysis by differential scanning calorimetery of empty lipid microparticles show a smallendothermic peak, corresponding to a polymorphic phase transition, at ~50°C and a melting endothermic peak at ~72°C, consistent with literature values (24,41). Similar patterns of peaks are visible

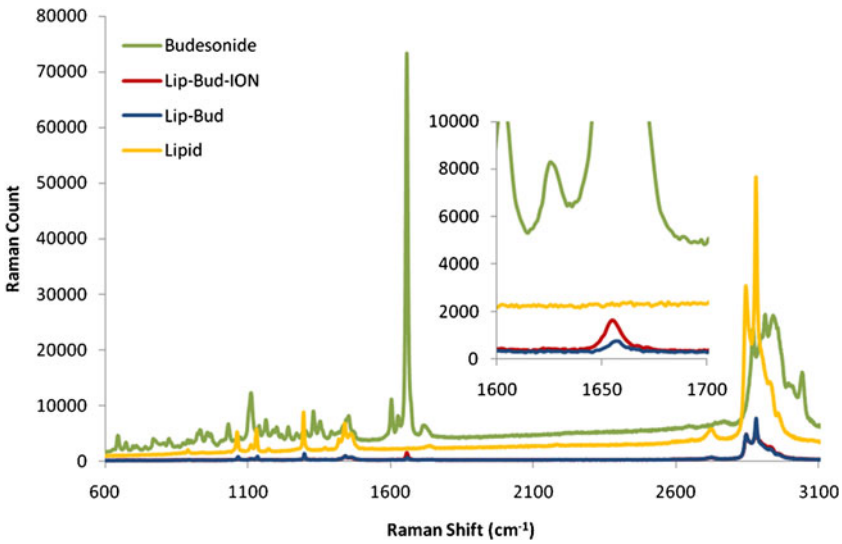

Fig. 5 Raman Spectra of budesonide, lipid, Lip-Bud and Lip-Bud-SPION formulations. *Inset* is magnified region between 1600 and 1700 cm^{-1} Raman shifts for clarification of budesonide peak at 1653 cm^{-1} in Lip-Bud and Lip-Bud-SPION formulations.

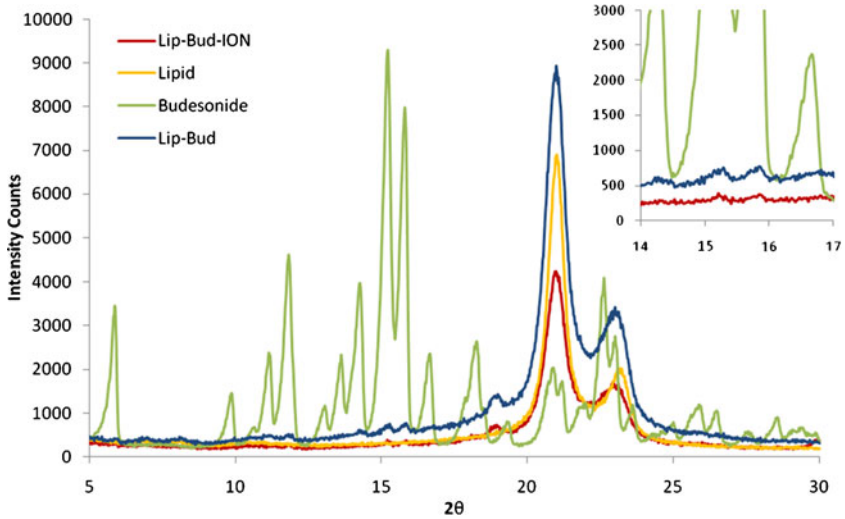

Fig. 6 X-ray powder diffraction spectra of free budesonide, and lipid, Lip-Bud and Lip-Bud-SION microcapsules. Inset: Magnification of the region between 14 and 17 2θ, with lipid graph omitted for ease of identifying the peaks corresponding to budesonide in the Lip-Bud and Lip-Bud-SPION microcapsules.

in both Lip-Bud and Lip-Bud-SPION microcapsules, with the small endothermic peak at ~50°C being sharper than that of the pure lipid. Crystalline budesonide has an exothermic crystallisation peak at 110°C and an endothermic melting peak at 259°C, neither of which were observed in the DSC traces of the Lip-Bud or Lip-Bud-SPION microcapsules, which was expected because drug is soluble in the lipid which melted at significantly lower temperature than the drug melting point.

Finally, inclusion of the SPIONs inside the Lip-Bud-SPION was confirmed using energy-dispersing X-ray spectroscopy (Fig. 7). Interestingly, the most intense signals come from the core of damaged lipid microparticles (shown in Fig. 7). Intact lipid particles around the damaged structure, showed very weak, if any, signals of iron.

In summary, vibrational spectroscopy confirmed the presence of budesonide in Lip-Bud and Lip-Bud-SPION microcapsules. Raman spectroscopy has a spot size of 1 μm. Thus, based on the area scanned, budesonide was present on the surface and/or within 1 μm depth into of the microparticles (42). Furthermore, Raman spectroscopy is a qualitative molecular fingerprinting technique. Thus the area under the peak, or peak height, is not a clear quantitative measure of budesonide concentration. Although the low peaks in the Lip-Bud and Lip-Bud-SPION samples are due to their low budesonide concentration, an amount of encapsuled drug cannot be accurately determined. XRD further confirmed the presence of budesonide within/on the lipid microcapsules. Limited signal from crystalline budensonide could be a result of either the rapid cooling of emulsion, freeze-drying process or long-term storage conditions (24,41). We have reported the presence of budesonide XRD peak in rapidly cooled spray-dried lipid only formulations (24) and thus the peak, in this case, is most likely due to the rapid cooling which results in primarily β′ and sub-α polymorphic mixtures of lipid (24). Independent studies assessing each effect: rapid cooling, freeze-drying and long-term storage, are required to establish the cause of such a peak.

Thermal analyses also indicated that budesonide became miscible with lipid phase and was completely integrated into the lipid matrix rather than crystallising outside of the lipid molecules (24). This test together, with Raman and XRD spectra confirm, that budesonide was integrated with the lipid matrix. Such complete encapsulation of budesonide into the lipid microparticles is desired as budesonide present outside of the microparticles would result in neither targeted, nor controlled release therapy.

The lipid-budesonide formulation was prepared at 90°C, which could potentially affect drug stability. Studies by Gupta (43) demonstrated that there is very little degradation of budesonide either by heat, oxidation or acid hydrolysis. In addition, our chemical analysis by Raman showed that there was no shift of the position of main peaks, which indicates that the structure of the drug was preserved. While this methodology cannot be applied for heat sensitive drugs, many anticancer therapies

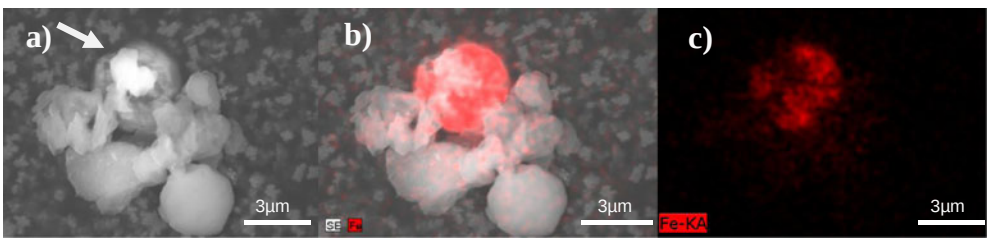

Fig. 7 (**a**) SEM image of Lip-Bud-SPION with arrow pointing to the damaged particles, (**b**) SEM image with iron signals detected in red and (**c**) map of iron distribution within the region.

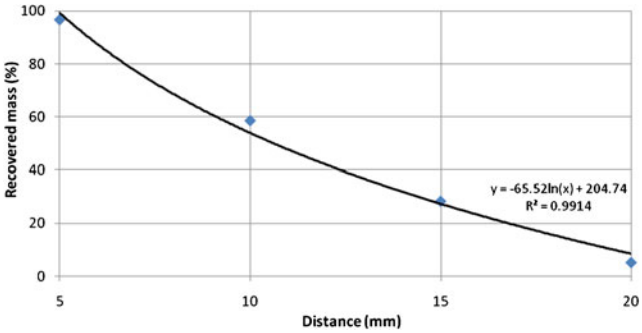

Fig. 8 Lip-Bud-SPION microparticle mobility under an applied magnetic field using three rare-earth magnets with a total surface magnetic force of 2194 gauss, over distances of 5 to 20 mm.

such as Paclitaxel or cisplatin, are generally considered thermally stable at increased temperatures (44,45).

For the purpose of formulating magnetically targeted and controlled release therapy, confirming the presence of SPIONs inside the lipid matrix was important. EDX was used to determine the presence and location of SPIONs in the Lip-Bud-SPION microparticles.

Magnetic Mobility Test

The ability of the Lip-Bud-SPION microparticles to move under magnetic influence was examined using a magnetic mobility test. Mass extraction was almost 100% when the magnet was placed at a distance of 5 mm from the microparticles with a ABST barrier in between (Fig. 8). As distance increased, the percentage extraction decreased logarithmically, in a first order release fashion, to ~5% at a distance of 2 cm. This suggested a need for more powerful magnet then simple earth magnets (used in this study) for targeted lung therapy.

Magnetic mobility test demonstrated that if the SPIONs were not encapsulated, or if they were loosely attached or loosely embedded into the lipid microcapaules such that they would detach from the matrix to move in response to the magnetic field, the maximum extraction fraction would have been approximately equal to the *w*/*w*% of SPION in the formulation (5%). Seeing close to 100% extraction at 5 mm, suggests that the entire particle is movable using a magnetic field and not just the SPIONs. The rare-earth magnets used in this study had a relatively weak surface magnetic field strength of 2194 gauss. Although such quantitative studies have not been performed previously, there are reports of substantial decreases in particle movement with the distance between similar iron nanoparticles and the magnets are increased just a few millimetres (8,17). In light of this, the greater extraction of the Lip-Bud-SPIONS (50%) at a distance of 1 cm from the magnet is a substantial improvement to previously reported formulations (46). It is normal that the magnetic actuation is attenuated with distance, but it was important demonstration of particles mobility using simple earth magnet even at specific distance.

There are already some reports that suggest using magnetic field it is possible to target cancer cells (47,48). In general, pulmonary delivery of aerosolised chemotherapy for the local treatment of lung tumours could be useful to (i) concentrate toxic agents at the tumour site only and (ii) avoid both systemic toxicities and invasive administration methods (49). Directing the chemotherapy of interest directly to the lung is advantageous and is likely to increase its efficacy and reduce systemic side effects. Intravenously delivered chemotherapy agents are diluted in systemic circulation, which results in a significant drop in the concentration of the drug that reaches the target tumour site (49). Since cancers must be treated chronically with various types of cytotoxic and/or cytostatic drugs. Furthermore, the repeated parenteral administration it leads to severe discomforts due to chronic the administrations.

However some problems associate with reaching pulmonary cancer tissue through inhalation have been shown (49), mostly due to the difficulties in the apparatuses used to deliver drugs to the lungs. Although problems have ben encountered, this technique has been able to achieve an adequate concentration and to eradicate the tumor sites. Thus pulmonary delivery holds a great promise to improve the effects of anticancer therapy, while reducing its severe side effects.

In the study Fe_3O_4 particles, which show very strong paramagnetism, were used. The mobility of the particles formulated with iron oxide was tested with earth magnets.

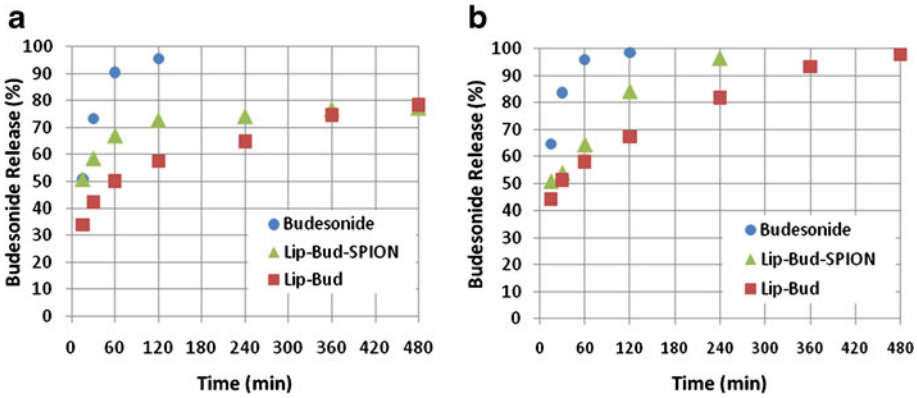

Fig. 9 *In vitro* diffusion/dissolution release profile of budesonide from budesonide only, and Lip-Bud and Lip-Bud-SPION microparticles at (**a**) 37°C a nd (**b**) 45°C, in phosphate buffer solution.

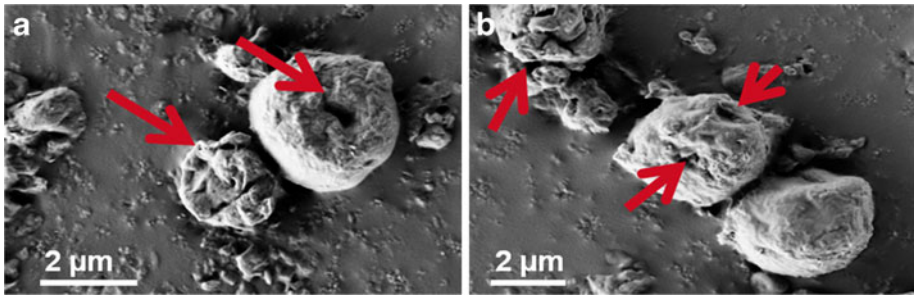

Fig. 10 SEM images of (**a**) Lip-Bud and (**b**) Lip-Bud-SPION particles after diffusion/dissolution test at 45°C, with arrows pointing to the damaged regions of the microcapsules.

The magnetic field generated by such magnets is typically of lower magnitude than the field generated by electromagnets, which are intended for the therapy. Therefore, the demonstration of the particles mobility with earth magnets ensures that the targeting can be enhanced and easily achieved using electromagnets. Further studies at higher SPION concentrations with stronger magnetic fields and real-size lung models might be necessary. Therapeutically useful particles need to be highly responsive to electromagnetic fields at 10-fold greater distances as human lungs have a cross-sectional length of 10–15 cm.

In Vitro Diffusion/Dissolution

Release of budesonide from the microparticles was examined under different conditions. The release profile of budesonide from budesonide only, Lip-Bud and Lip-Bud-SPION formulations at body temperature (37°C) and hyperthermic temperature (45°C). Complete release of budesonide from budesonide only samples was achieved within 2 h at 37°C, while the release of budesonide from Lip-Bud and Lip-Bud-SPION microparticles only reached a maximum of 80% after 8 h (Fig. 9a).

Budesonide release from Lip-Bud microparticles reached close to 95% at the end of 6 h and close to 100% after 8 h at 45°C. Budesonide release from Lip-Bud-SPION reached more than 95% just after 4 h. The release of the drug from budesonide-only formulation was similar to previous experimented data collected at 37°C.

An attempt to characterise the mechanism of drug release/dissolution diffusion models that best fitted the release profile of the three samples at both two different temperatures were examined. The R^2 value obtained from regression analysis of each release profile for the five most popular diffusion mechanisms (Zero-order, first-order, Higuchi,Hixson-Crowell, Korsmeyer-Peppas) showed that only budesonide followed first order release kinetics at both 37°C and 45°C. Interestingly, at 45°C, the Lip-Bud-SPION microparticles matched first order release kinetics, which was not observed for the Lip-Bud microparticles (Fig. 9b). At 37°C both the Lip-Bud and Lip-Bud-SPION followed Korsmeyer-Peppas mechanism. Scanning electron microscope images showed damaged, or disintegrated, lipid microparticles for both Lip-Bud and Lip-Bud-SPION after 8 h incubation at 45°C suggesting microparticle degradation as the mechanism of the release, rather than simple diffusion through the lipid coating (Fig. 10). Having no other external structure obstructing its release, the release of budesonide was solely dependent on its diffusion across the concentration gradient, thus resulting in first order release kinetic. Lip-Bud and Lip-Bud-SPION microparticles best matched Korsmeyer-Peppas release kinetics, which

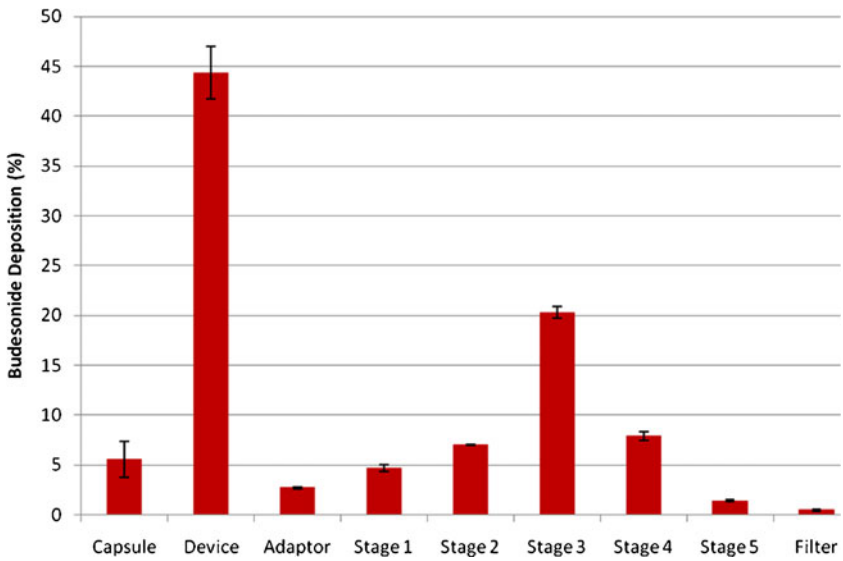

Fig. 11 *In vitro* aerosol performance of Lip-Bud-SPION microcapsules, measured on a Marple-miller cascade impactor, showing a total fine particle fraction of 30 ± 1.15% (n=2).

describes release from complex, polymer-like, erosion controlled release systems (50). This was expected as insoluble lipid has a transition temperature at 50°C, with the onset being at around 42–45°C and thus would erode slowly upon heating and thus act as the rate limiting step for budesonide dissolution. The easy penetration of the media through the holes in particles is also likely to have contributed to the first order budesonide release.

Assuming that a temperature of 45°C is feasible to achieve drug release from the Lip-Bud-SPION microparticles by the application of external stimuli, it should be possible to achieve controlled release of the drug *in vivo*. It is very likely that if the increase in temperature is achieved by alternating magnetic field which results in mechanical agitation the release process would be further enhanced. This phenomena would be highly desired—external stimulation.

In Vitro Dry Powder Aerosol Performance

Although the geometric and volumetric diameters of the Lip-Bud and Lip-Bud-SPION microparticles are less than 5 μm, lung deposition relies upon the aerodynamic diameter of the particles and the performance of the dry-powder from the inhaler device. The design of the Marple-Miller cascade impacter allows capture of particles with aerodynamic diameters greater than 10, 5, 2.5, 1.25 and 0.625 μm in stages 1, 2, 3, 4 and 5, respectively. A fine particle fraction percentage (FPF < 5 μm, drug deposited at stages 3–5 and on the filter) of 30 ± 1.15% was achieved (Fig. 11).

Importantly, aerosol performance studies confirmed higher performance of the Lip-Bud-SPION microparticles when compared to marketed control inhalation formulations (51). We hypothesise that the excellent performance of the Lip-Bud-SPION may be due to charge interactions between the plastic Aerolizer™ device and the microcapsules. This phenomena was previously shown to impact on inhalers performance (52).

SUMMARY AND CONCLUSIONS

Targeted and controlled drug delivery are two key research areas across many disciplines. In particular anticancer therapy requires closely controlled targeting and drug release to avoid harmful side effects. This is also true for other therapies, which can benefit from novel thermally activated and magnetically guided delivery systems, as developed here. Achieving effective magnetic guidance with controlled drug release will be a major milestone in drug delivery research. It is particularly important in lung drug delivery, where limited responsiveness to current approaches to guide and trigger drug release has been achieved. This research focussed on the development of lipid-based drug delivery systems utilising super paramagnetic iron nanoparticles that may allow targeted delivery using magnetic fields. Drug release was stimulated by an increase in temperature to 45°C.

In conclusion, a model drug and SPION loaded lipid system of desired physical-chemical characteristics, with relatively high aerosol performances, was formulated using optimised oil in water emulsion technique. The lipid system was thermo-sensitive, allowing slow drug release at body temperature, but fast release at hyperthermic temperature. The drug-lipid-SPION system was magnetically active and movable using simple rare-earth magnets. The formulated drug-delivery system, holds a promise as an effective drug vehicle in targeted and controlled inhalation therapy. The drug and SPIONS were (i) successfully incorporated into lipid microparticles, (ii) they have optimal size for inhalation therapy, (iii) the microparticles were magnetic sensitive, and (iv) thermo-sensitive that allowed controlling drug release.

REFERENCES

1. Lubbe AS, Alexiou C, Bergemann C. Clinical applications of magnetic drug targeting. J Surg Res. 2001;95(2):200–6.
2. Organization, W.H., *Cancer*, in *Fact sheet N°297*. 2009.
3. Silvestri GA, Alberg AJ, Ravenel J. The changing epidemiology of lung cancer with a focus on screening. Br Med J. 2009;339 (b3053):451–4.
4. Limited TG, *Therapeutic Guidelines: Respiratory*. Therapeutic Guidelines, ed. T.G. Limited. Vol. 3. 2005, Melbourne. 210.
5. Martin AR, Finlay WH. Alignment of magnetite-loaded high aspect ratio aerosol drug particles with magnetic fields. Aerosol Sci Technol. 2008;42:295–8.
6. Martin AR, Finlay WH. Enhanced deposition of high aspect ratio aerosols in small airway bifurcations using magnetic field alignment. J Aerosol Sci. 2008;39(8):295.
7. Gupta AK, *et al.* Synthesis and surface engineering of iron oxide nanoparticles for biomedical applications. Biomaterials. 2005;26 (18):3995–4021.
8. Douziech-Eyrolles L, *et al.* Nanovectors for anticancer agents based on superparamagnetic iron oxide nanoparticles. Int J Nanomedicine. 2007;2(4):541–50.
9. Amirfazli A, Amirfazli A. Nanomedicine: magnetic nanoparticles hit the target. Nat Nanotechnol. 2007;2(8):467–8.
10. Veiseh O, *et al.* Design and fabrication of magnetic nanoparticles for targeted drug delivery and imaging. Adv Drug Deliv Rev. 2010;62(3):284–304.
11. Cunningham CH, *et al.* Positive contrast magnetic resonance imaging of cells labeled with magnetic nanoparticles. Magn Reson Med. 2005;53(5):999–1005.
12. Anderson SA, *et al.* Magnetic resonance contrast enhancement neovasculature with α(v)β3-targeted nanoparticles. Magn Reson Med. 2000;44(3):433–9.
13. Polyak B, Friedman G. Magnetic targeting for site-specific drug delivery: applications and clinical potential. Expert Opin Drug Deliv. 2009;6(1):53–70.
14. Jalilian AR, *et al.* Preparation and biological evaluation of [67Ga]-labeled- superparamagnetic nanoparticles in normal rats. Radiochim Acta. 2009;97(1):51–6.

15. Talelli M, *et al.* Superparamagnetic iron oxide nanoparticles encapsulated in biodegradable thermosensitive polymeric micelles: toward a targeted nanomedicine suitable for image-guided drug delivery. Langmuir. 2009;25(4):2060–7.
16. Shubayev VI, Pisanic TR, Jin S. Magnetic nanoparticles for theragnostics. Adv Drug Deliv Rev. 2009;61(6):467–77.
17. Jain TK, *et al.* Biodistribution, clearance, and biocompatibility of iron oxide magnetic nanoparticles in rats. Mol Pharm. 2008;5(2):316–27.
18. Soenen SJ, *et al.* Cellular toxicity of inorganic nanoparticles: common aspects and guidelines for improved nanotoxicity evaluation. Nano Today. 2011;6(5):446–65.
19. Neuberger T, *et al.* Superparamagnetic nanoparticles for biomedical applications: possibilities and limitations of a new drug delivery system. J Magn Magn Mater. 2005;293(1):483–96.
20. Kettering M, *et al.* Characterization of iron oxide nanoparticles adsorbed with cisplatin for biomedical applications. Phys Med Biol. 2009;54(17):5109–21.
21. Dames P, *et al.* Targeted delivery of magnetic aerosol droplets to the lung. Nat Nanotechnol. 2007;2(8):495–9.
22. Son Y-J, McConville JT. Advancements in dry powder delivery to the lung. Drug Dev Ind Pharm. 2008;34(9):948–59.
23. Reddy LH, *et al.* Tamoxifen citrate loaded solid lipid nanoparticles (SLN): preparation, characterization, *in vitro* drug release, and pharmacokinetic evaluation. Pharm Dev Technol. 2006;11 (2):167–77.
24. Mezzena M, *et al.* Solid lipid budesonide microparticles for controlled release inhalation therapy. AAPS J. 2009;11(4):771–8.
25. Weyhers H, *et al.* Solid lipid nanoparticles (SLN)–effects of lipid composition on *in vitro* degradation and *in vivo* toxicity. Pharmazie. 2006;61(6):539–44.
26. Sanna V, *et al.* Preparation and *in vivo* toxicity study of solid lipid microparticles as carrier for pulmonary administration. AAPS PharmSciTech. 2004;5(2):e27.
27. Patton JS, Byron PR. Inhaling medicines: delivering drugs to the body through the lungs. Nat Rev Drug Discov. 2007;6(1):67–74.
28. Salama RO, *et al.* Preparation and characterisation of controlled release co-spray dried drug-polymer microparticles for inhalation 2: evaluation of *in vitro* release profiling methodologies for controlled release respiratory aerosols. Eur J Pharm Biopharm. 2008;70(1):145–52.
29. Salama RO, *et al.* Preparation and characterisation of controlled release co-spray dried drug-polymer microparticles for inhalation 2: evaluation of *in vitro* release profiling methodologies for controlled release respiratory aerosols. Eur J Pharm Biopharm. 2008;70(1):145–52.
30. Young PM, *et al.* Recent advances in understanding the influence of composite-formulation properties on the performance of dry powder inhalers. Physica B. 2007;394(2):315–9.
31. Martonen TB, *et al.* Issues in drug delivery: concepts and practice. Respir Care. 2005;50(9):25.
32. Bhavsar MD, Tiwari SB, Amiji MM. Formulation optimization for the nanoparticles-in-microsphere hybrid oral delivery system using factorial design. J Control Release. 2006;110(2):422–30.
33. Heslinga MJ, Mastria EM, Eniola-Adefeso O. Fabrication of biodegradable spheroidal microparticles for drug delivery applications. J Control Release. 2009;138(3):235–42.
34. Sturesson C, *et al.* Encapsulation of rotavirus into poly(lactide-co-glycolide) microspheres. J Control Release. 1999;59(3):377–89.
35. Sowerby SJ, Broom MF, Petersen GB. Dynamically resizable nanometre-scale apertures for molecular sensing. Sensors Actuators B Chem. 2007;123(1):325–30.
36. Willmott GR, *et al.* Use of tunable nanopore blockade rates to investigate colloidal dispersions. J Phys Condens Matter. 2010;22 (45):454116.
37. Roberts GS, *et al.* Tunable nano/micropores for particle detection and discrimination: scanning ion occlusion spectroscopy. Small. 2010;6(23):2653–8.
38. Vogel R, *et al.* Quantitative sizing of nano/microparticles with a tunable elastomeric pore sensor. Anal Chem. 2011;83(9):3499–506.
39. Ali HRH, *et al.* Vibrational spectroscopic study of budesonide. J Raman Spectrosc. 2007;38(7):903–8.
40. Jores K, *et al.* Solid lipid nanoparticles (SLN) and oil-loaded SLN studied by spectrofluorometry and Raman spectroscopy. Pharm Res. 2005;22(11):1887–97.
41. Hamdani J, *et al.* Physical and thermal characterisation of Precirol and Compritol as lipophilic glycerides used for the preparation of controlled-release matrix pellets. Int J Pharm. 2003;260(1):47–57.
42. Renishaw P. *How Renishaw's inVia Raman system provides high spectral resolution from a 250 mm focal length spectrometer*. Technology note from the Spectroscopy Products Division, 2005(1).
43. Gupta M, Bhargava HN. Development and validation of a high-performance liquid chromatographic method for the analysis of budesonide. J Pharm Biomed Anal. 2006;40(2):423–8.
44. Poklar N, *et al.* Influence of cisplatin intrastrand crosslinking on the conformation, thermal stability, and energetics of a 20-mer DNA duplex. Proc Natl Acad Sci. 1996;93(15):7606–11.
45. Montaseri H, *et al.* The effect of temperature, ph, and different solubilizing agents on stability of taxol. Iranian J Pharm Sci. 2004;1(1):8.
46. Jordan A. *Hyperthermia classic commentary: ' Inductive heating of ferrimagnetic particles and magnetic fluids: Physical evaluation of their potential for hyperthermia' by Andreas Jordan et al., International Journal of Hyperthermia, 1993;9:51–68*. Vol. 25. 2009. 512–6.
47. Veiseh O, Gunn JW, Zhang M. Design and fabrication of magnetic nanoparticles for targeted drug delivery and imaging. Adv Drug Deliv Rev. 2010;62(3):284–304.
48. Veiseh O, *et al.* Cancer cell invasion: treatment and monitoring opportunities in nanomedicine. Adv Drug Deliv Rev. 2011;63 (8):582–96.
49. Wauthoz N, *et al. In vivo* assessment of temozolomide local delivery for lung cancer inhalation therapy. Eur J Pharm Sci. 2010;39 (5):402–11.
50. Shoaib MH, *et al.* Evaluation of drug release kinetics from ibuprofen matrix tablets using HPMC. Pak J Pharm Sci. 2006;19(2):119–24.
51. Joshi MR, Misra A. Liposomal budesonide for dry powder inhaler: preparation and stabilization. AAPS PharmSciTech. 2001;2(4):25.
52. Hoe S, Young PM, Traini D. A review of electrostatic measurement techniques for aerosol drug delivery to the lung: implications in aerosol particle deposition. J Adhes Sci Technol. 2011;25(4–5):385–405.